René Lindell, Jari Penttilä, Mika Sillanpää, and Pertti Hakonen, Quantum states of a mesoscopic SQUID measured using a small Josephson junction, Physical Review B 68, 052506 (2003).

© 2003 American Physical Society.

Reprinted with permission.

Readers may view, browse, and/or download material for temporary copying purposes only, provided these uses are for noncommercial personal purposes. Except as provided by law, this material may not be further reproduced, distributed, transmitted, modified, adapted, performed, displayed, published, or sold in whole or part, without prior written permission from the publisher.

PHYSICAL REVIEW B **68**, 052506 (2003)

Quantum states of a mesoscopic SQUID measured using a small Josephson junction

René Lindell, Jari Penttilä, Mika Sillanpää, and Pertti Hakonen
Low Temperature Laboratory, Helsinki University of Technology, FIN-02015 HUT, Finland
(Received 19 March 2003; published 19 August 2003)

We have experimentally studied the energy levels of a mesoscopic superconducting quantum interference device (SQUID) using inelastic Cooper-pair tunneling. The tunneling in a small Josephson junction depends strongly on its electromagnetic environment. We use this fact to do energy-level spectroscopy of a SQUID loop by coupling it to a small junction. Our samples with strong quasiparticle dissipation are well described by a model of a particle localized in one of the dips in a cosine potential, while in the samples with weak dissipation we can see formation of energy bands.

DOI: 10.1103/PhysRevB.68.052506 PACS number(s): 74.50.+r, 73.23.Hk

The Josephson junction, despite its simple structure, has proven to be surprisingly versatile and new applications are found in quantum computing and nanoelectronics.[1,2] The devices are based on the quantum-mechanical behavior of the superconducting phase variable,[3] which has been previously studied with either rf irradiation[4] or during rapid current ramping.[5,6] We are using a different probe, namely, an additional mesoscopic Josephson junction. Our scheme is based on the theory of phase fluctuations,[7,8] according to which Coulomb blockade in a single superconducting tunnel junction is strongly affected by its environment. Noncoherent Cooper pair tunneling is allowed only if energy is exchanged with the surroundings. Thus, this inelastic Cooper pair tunneling provides a good tool for observing all kinds of environmental modes in a rather simple fashion.[9]

In this paper, we present detailed spectroscopic investigations on small SQUID loops, which are driven from the nearly classical limit ($E_J/E_C \gg 1$) deep into the quantum regime ($E_J/E_C \sim 1$). Our results yield evidence for higher-energy bands of the macroscopic phase variable in a regime ($E_J/E_C \gtrsim 1$) where they have not been investigated before.[10] In addition, our experiment provides the verification that multiphoton transitions involving separate quantum-mechanical harmonic oscillators do play a role in electron tunneling in a mesoscopic tunnel junction.

As an energy detector in our measurement we use a voltage biased, superconducting tunnel junction which has a smaller size and critical current than the junction we want to study. For large (conventional) Josephson junctions, the supercurrent is given by $I=I_c\sin(\varphi)$, where I_c is the critical current, which is related to the Josephson coupling energy $E_J=\hbar I_C/(2e)$. The phase $\varphi(t)=\int_{-\infty}^{t}(2e/\hbar)V(t')dt'$ is defined as an integral of the voltage V across the tunnel barrier. For small junctions, where the charging energy $E_C=e^2/(2C) \gg E_J$ Cooper pair tunneling is inelastic and given by

$$I(V)=\frac{\pi e E_J^2}{\hbar}[P(2eV)-P(-2eV)], \qquad (1)$$

where $P(E)$ is a function describing the probability of energy exchange between a tunnel junction and its electromagnetic environment and depends on the impedance seen by the junction.[8]

At low temperatures, the junction environment, i.e., the heat bath, is in its ground state and $P(E)\simeq 0$ for $E<0$. Thus, the latter term in Eq. (1) can be neglected and $I(V)$ becomes directly proportional to $P(2eV)$. The theory is valid for linear impedances constructed from lumped elements. Nevertheless, we argue that the idea of energy exchange can be generalized so that a discrete spectrum of energy levels in the environment will cause a set of discrete peaks in the IV curve. Hence, the small detector junction can be used for spectroscopy.

A Josephson junction can be described by the Schrödinger equation[11]

$$\frac{d^2\psi(\varphi)}{d(\varphi/2)^2}+\left(\frac{E}{E_c}+\frac{E_J}{E_c}\cos\varphi+\frac{I}{I_C}\varphi\right)\psi(\varphi)=0, \qquad (2)$$

where I is the current flowing through the junction. The current in our measurements always satisfies $I \ll I_C$, so the tilt in the potential is negligible and setting $I=0$ in Eq. (2) leads to the familiar Mathieu equation. The single junction Hamiltonian can also be used to describe a SQUID loop, where the loop size is so small that the geometric inductance can be neglected and the loop is perfectly symmetric. The only difference is that E_J then depends periodically on an externally applied magnetic flux Φ according to $E_J=2E_J^{single}|\cos(\pi\Phi/\Phi_0)|^2$, where $\Phi_0=h/(2e)$ and E_J^{single} is the Josephson coupling energy for a single junction. For large E_J/E_C, the particle is trapped in one of the potential wells. In this case, for currents $I \ll I_C$, the Josephson junction can be described by an inductance $L=\Phi_0/(2\pi I_c)$. Combined with the capacitance of the tunnel junction, the junction forms an LC oscillator with a characteristic resonance frequency of $\omega_p=1/\sqrt{LC}=\sqrt{8E_JE_c}/\hbar$. Consequently, a Josephson junction behaves like a harmonic oscillator with a level spacing of ω_p. When E_J/E_C becomes smaller, the energy levels are not harmonic but they will depend on the shape of the cosine potential.

Depending on the environmental resistance seen by the Josephson junction, i.e., in our case "the environment of the environment," the junction can become completely delocalized and the whole periodicity of the cosine potential has to be accounted for.[12,11] The eigenstates are then given by Bloch functions $\Psi_n(\varphi)=u_n(\varphi)e^{i\varphi q/(2e)}$, where q is the qua-

 ©2003 The American Physical Society

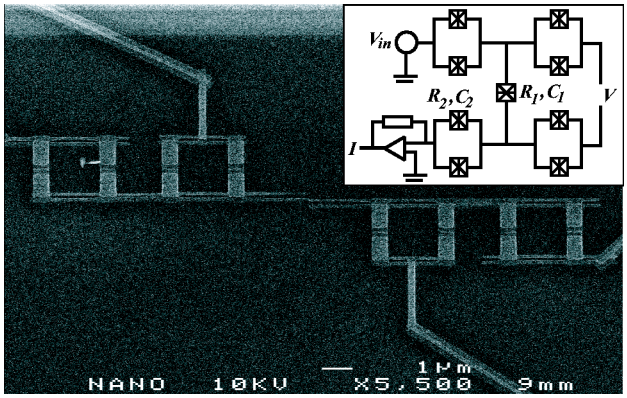

FIG. 1. SEM micrograph of a sample with four SQUID's. The probe junction has an area of 100×100 nm^2 and the SQUID junctions 150×550 nm^2 In the samples covered in this paper, additional gate leads were available for the islands. Inset shows the schematic of the circuit in the 4-lead measurement.

sicharge, n is the band index, and $u_n(\varphi)$ is a 2π-periodic function. This phase transition from the localized to delocalized state happens when $R>R_Q$, where $R_Q=h/(4e^2)$, or 6.45 kΩ .[13,14] In our measurement, we need a clear voltage bias and thus we have not fabricated any resistor close to the junction. The source of dissipation is, therefore, given by the quasiparticle resistance of the probe junction. This changes the periodicity of the wave functions from 2π to 4π and each band is split into two.[12]

We have carried out experiments with different circuit configurations; both 2- and 4-lead measurements including 1, 2, or 4 SQUID(s) coupled to a small detector junction. We will here describe measurements of two different samples; a 4-SQUID sample with four leads and a 1-SQUID sample with just two leads. A scanning electron micrograph (SEM) of the 4-SQUID sample, together with a schematic drawing of the same, is shown in Fig. 1. The SQUID configuration allows us to change the energy levels of the measured system and enables us to resolve the resonances due to the SQUID(s) from other resonances in the environment. The critical current, or equally, the value of E_J could be tuned to less than 1% of the maximum, which shows that our SQUID's were very homogeneous. For the 4-SQUID sample, the critical currents for individual SQUID's were within 2.5% from the average value. The samples were made from aluminum with *e*-beam lithography and two-angle evaporation in an UHV chamber.

The four-wire setup facilitates the determination of circuit parameters. The important parameters are E_J and E_C, or rather their ratio. The Ambegaokar-Baratoff (A-B) formula, $E_J=\hbar\pi\Delta/(4e^2R_T)$, was used to find E_J from the normal-state resistances R_T, while the capacitances were estimated from the junction areas (see Fig. 1) using a value of 45 fF/μm^2.[15] The BCS-gap Δ was about 215 μeV in our samples. The experimental parameters for the different circuits are summarized in Table I.

The samples were mounted into a rf-tight copper enclosure and cooled down to 80 mK with a plastic dilution refrigerator. The measurement leads were filtered using 0.7-m-long sections of Thermocoax. Minicircuits rf filters with a cutoff frequency of 1.9 MHz were employed on the top of the cryostat at room temperature.

TABLE I. Parameters for the 4-SQUID and 1-SQUID samples. Energies are given in units of μeV. The Ambegaokar-Baratoff values for E_J are given in parentheses.

Sample	R_T (kΩ)	C(fF)	E_J	E_C	E_J/E_C
4-SQUID (detector)	166	0.5	3.6	160	0.023
4-SQUID (SQUID)	2.5	7.6	544 (272)	10.5	51.8
1-SQUID (detector)	70	0.8	8.5	100	0.08
1-SQUID (SQUID)	3.5	5.7	422 (188)	14	30.1

Figure 2 displays the measured IV curve for zero magnetic flux, or maximum E_J, for the 4-SQUID sample together with an IV curve simulated with $P(E)$ theory. The locations of the peaks were found to depend only on the magnetic flux, not at all on the gate voltages. To properly identify the energy levels of the SQUID, we measure IV curves for different magnetic fields. The peak positions as function of applied flux are shown in Fig. 3.

The width of the resonance peaks (about 4 μeV) is smaller than $k_BT=7$ μeV. The width is therefore either intrinsic or given by external noise. Our peak widths are thus comparable to or even smaller than what has been observed in similar spectroscopic studies.[16]

The peak structure can be qualitatively explained with a three-resonator model, where one resonator represents all the SQUID's and the two other come from the rest of the measurement circuitry; bonding wires and pads. The parameters of the simulation and simulation circuitry are found in Fig. 2. The parameters for the SQUID were taken from the 2 lead measurement involving only two SQUID's in series, but the

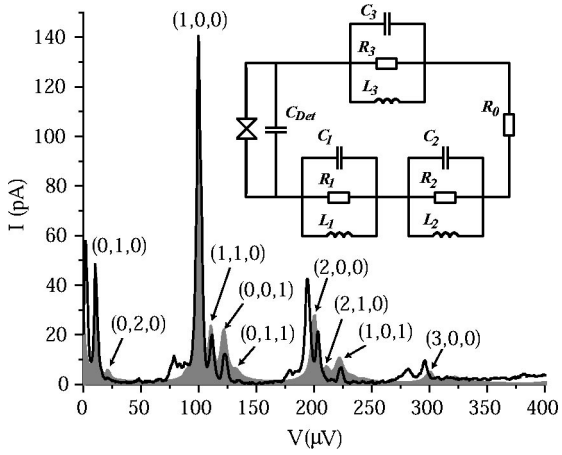

FIG. 2. IV-curve for the 4-SQUID sample at maximum E_J and the circuit model used in simulation. The full line shows the experimental curve while the shaded area shows the simulated curve. The different excitations in the simulation are denoted as (n,k,l), where n,k, and l are the number of quanta excited. The first index gives the resonance due to SQUID's and the two other indices are due to other resonances in the circuit. The parameters used in the simulation are $C_{Det}=0.5$ fF, $C_1=4$ fF, $L_1=2.28$ nH, $R_1=50$ kΩ (SQUID), $C_2=0.5$ pF, $L_2=3.2$ nH, $R_2=30$ kΩ, $C_3=2$ fF, $L_3=10.8$ nH, $R_3=3$ kΩ, $R_0=100$ Ω, and $T=100$ mK.

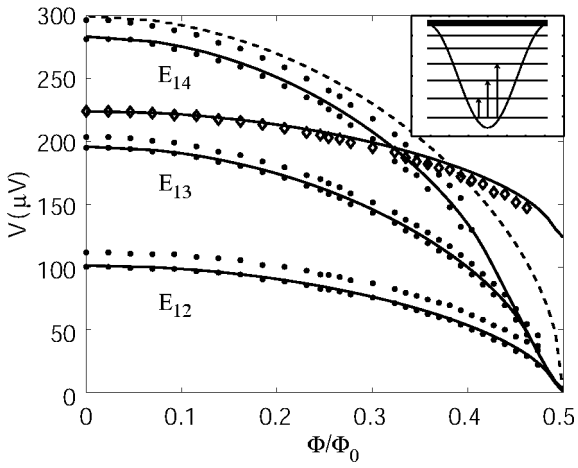

FIG. 3. The position of the main resonances as a function of applied flux for the 4-SQUID sample and the calculated transitions. The main resonances due to the SQUID loops consist of a double-peak structure. The potential well and the energy levels and shown in the inset. The arrows indicate the transitions that are clearly seen in the experiment. To compare with a harmonic potential, the transition from first to fourth harmonic is indicated by the dashed line. The multiphoton process (1,0,1) is shown by the diamonds.

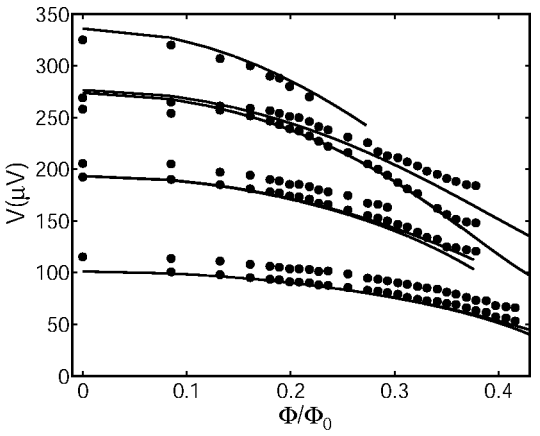

FIG. 4. Positions of the measured resonances for the 1-SQUID sample and the theoretical transitions between band edges when the wave functions are 4π periodic. The resonances are grouped into four groups, which are transitions between bands $1\rightarrow2$, $1\rightarrow3$, $1\rightarrow4$, and $1\rightarrow5$. As in the 4-SQUID sample, there is a double-peak structure which it not explained by the model.

parameters of the two other resonator circuits were fitted to *IV* curve. The resistances used in the simulation represent the broadening of peaks due to dissipation and noise.

The $P(E)$ function in Eq. (1) was calculated using the integral equation approach presented in Ref. 17. The comparison of the *IV* curve with the simulation indicates that the sequence of multiphoton peaks of a harmonic oscillator [(1,0,0), (2,0,0), and (3,0,0)] nearly agrees with the measured shape. However, the energy levels are not exactly equally spaced as would be the case for a classical inductance.

In order to find a better quantitative agreement with the level spacing, the Schrödinger equation (2) was numerically solved under the assumption that the particle is localized in one of the wells. The experimental peaks together with the calculated transitions are shown in Fig 3. The form of the cosine potential decreases the level spacing from the harmonic case. This deviation from the harmonic-oscillator case is largest for the third transition as can be seen in Fig. 3, where also the transition from the first to fourth harmonic level is shown for comparison. Peak (1,0,1) is clearly a multiphoton process (see Fig. 3), which is the sum of the flux-dependent transition in a SQUID (1,0,0) and the flux-independent transition (0,0,1).

The parameter for E_J used in the calculation is about twice the value given by the *A-B* relation (see Table I). Typically, E_J is expected to be renormalized downwards due to the low impedance environment, but in our case it is renormalized upwards. Similar disagreements between the *A-B* value have been reported before.[15,16] Our model does not, however, explain the double-peak structure (see Fig. 3) found in all the *IV* curves. This peak splitting is fairly constant over the whole measurement range, but the position of the double peak is different for the three main transitions. The doublet structure is observed also in circuits containing just a detector junction and one SQUID. Thus, we can rule out the asymmetry between different SQUID's as the origin of the doublets.

The two-point measurements with both one and two SQUID(s) showed similar behavior as the 4-SQUID measurements. The number of SQUID's in the sample did not seem to have any significant effect on the *IV* curve. Rather, there are notable differences between the 2-lead and 4-lead samples. In the 1-SQUID sample with only two leads, the current dropped very fast when tuning down E_J (from 360 pA at $\Phi/\Phi_0=0$ to 40 pA at $\Phi/\Phi_0=0.4$). This behavior can be explained when considering that the current through the circuit is given by two rates: the excitation of oscillator modes in the SQUID and their subsequent relaxation, which depends on the environment seen by the SQUID. In the 2-lead circuits, the current is limited by the down relaxation, and the effect can be approximatively explained with the formula[18]

$$\Gamma_{\downarrow}=2\sum_{l<n}\mathrm{Re}\{Y(E_{ln}/\hbar)\}(E_{ln}/\hbar)R_Q|\langle l|\varphi|n\rangle|^2, \qquad (3)$$

where the admittance is given by $Y(\omega)=[1/(i\omega C_{Det})+R_0]^{-1}$ and C_{Det} is the capacitance of the detector junction (0.8 fF) in series with the resistance of the environment, R_0 (100 Ω).

The positions of the clearest flux-dependent peaks for the 1-SQUID sample are shown in Fig. 4. In this case, better agreement with the measured resonances is found when considering the full periodicity of the cosine potential in Eq. (2). However, the value of E_J was taken to be twice the *A-B* value, as in the case with four SQUID's. This apparent enhancement of E_J is probably due to the charging energy, as discussed in Ref. 19. The effect according to the theory is, however, smaller than what we observe.

Because the transitions are due to transfer of Cooper pairs in the detector junction, the allowed first-order transitions can be found by calculating the matrix element $|\langle l|e^{-i\varphi}|n\rangle|$

between bands l and n. In addition, due to van-Hove-like singularities, the observed transitions are between band edges. The transition between the first and the fourth band is clearly visible as two distinct peaks. The lowest bands are so narrow that they only show up in the width of the resonance peaks. As the E_J/E_C ratio is tuned down, the lifetime of the states increases and this should lead to narrower peaks. But, instead we observe a broadening of the resonances, indicating a broadening of the bands as expected from theory.

The theory for Josephson junctions[12] tells that in order for band formation we need to suppress the ohmic or quasiparticle dissipation in the environment, which causes the phase to localize. In our system, this suppression is provided by the large quasiparticle resistance of the detector junction. Therefore, the wave functions are 4π-periodic and each band from the 2π-periodic case is split into two. The observed transitions are, however, the same as what would be expected for 2π-periodic bands. Consequently, the true periodicity of the bands cannot be resolved in the experiment.

In summary, we have experimentally studied the quantum-mechanical energy levels of the Josephson junction. Our results for samples with $E_J/E_C \gg 1$ can qualitatively be described by $P(E)$ theory involving multiphoton excitations. The nonlinearity of the SQUID systems, prominent of $E_J \sim E_C$, can be taken into account by considering the exact form of the cosine potential. Evidence of the existence of Bloch bands is observed in our 2-lead samples both in the form of van-Hoven-like singularities between band edges and a broadening of resonance peaks. Our results show that a small superconducting junction can be employed as a detector for mesoscopic quantum circuits.

Fruitful discussions with D. Haviland, F. Hekking, F. Wilhelm, G. Schön, J. Siewert, E. Thuneberg, A. Zaikin, and T. Heikkilä are gratefully acknowledged. This work was supported by the Academy of Finland and by the Large Scale Installation Program ULTI-3 of the European Union.

[1] D. Vion *et al.*, Science **296**, 886 (2002).
[2] J. Delahaye *et al.*, Science **299**, 1045 (2003).
[3] J. Clarke, A. Cleland, M. Devoret, D. Esteve, and J. Martinis, Science **239**, 992 (1988).
[4] M.H. Devoret, J.M. Martinis, and J. Clarke, Phys. Rev. Lett. **55**, 1908 (1985).
[5] P. Silvestrini, V.G. Palmieri, B. Ruggiero, and M. Russo, Phys. Rev. Lett. **79**, 3046 (1997).
[6] A. Wallraff, T. Duty, A. Lukashenko, and A.V. Ustinov, Phys. Rev. Lett. **90**, 037003 (2003).
[7] M.H. Devoret *et al.*, Phys. Rev. Lett. **64**, 1824 (1990).
[8] G.-L. Ingold and Yu. V. Nazarov, in *Single Charge Tunneling*, edited by H. Grabert and M. H. Devoret (Plenum Press, New York, 1992), p. 21.
[9] T. Holst, D. Esteve, C. Urbina, and M.H. Devoret, Phys. Rev. Lett. **73**, 3455 (1994).
[10] D.J. Flees, S. Han, and J.E. Lukens, Phys. Rev. Lett. **78**, 4817 (1997).
[11] K.K. Likharev and A.B. Zorin, J. Low Temp. Phys. **59**, 347 (1985); D.V. Averin, A.B. Zorin, and K.K. Likharev, Zh. Eksp. Teor. Fiz. **88**, 692 (1985) [Sov. Phys. JETP **61**, 407 (1985)].
[12] G. Schön and A.D. Zaikin, Phys. Rep. **198**, 237 (1990).
[13] J.S. Penttilä *et al.*, Phys. Rev. Lett. **82**, 1004 (1999).
[14] R. Yagi, S. Kobayashi, and Y. Ootuka, J. Phys. Soc. Jpn. **66**, 3722 (1997).
[15] D.B. Haviland and P. Delsing, Phys. Rev. B **54**, 6857 (1996).
[16] E. Bibow, P. Lafarge, and L.P. Lévy, Phys. Rev. Lett. **88**, 017003 (2002).
[17] G.-L. Ingold and H. Grabert, Europhys. Lett. **14**, 371 (1991).
[18] J.M. Martinis, M.H. Devoret and J. Clarke, Phys. Rev. B **35**, 4682 (1987).
[19] A.D. Zaikin, J. Low Temp. Phys. **88**, 373 (1992).